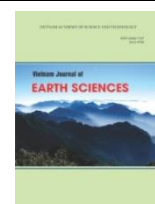




Vietnam Academy of Science and Technology  
**Vietnam Journal of Earth Sciences**  
<http://www.vjs.ac.vn/index.php/jse>



## Assessment and reduction of zenith path delay biases due to day boundary effect

Nguyen Ngoc Lau<sup>1,2</sup>, Richard Coleman<sup>3</sup>

<sup>1</sup>*Ho Chi Minh City University of Technology, Vietnam*

<sup>2</sup>*Vietnam National University Ho Chi Minh City, Vietnam*

<sup>3</sup>*University of Tasmania, Australia*

Received 31 May 2021; Received in revised form 15 September 2021; Accepted 27 October 2021

### ABSTRACT

The troposphere consists of dry air and water vapor, delaying the GNSS signal by about 2.4 m in the zenith direction. The water vapor only causes an error of about 0.2 m in distance measurement, but it is challenging to model and overcome. From 2003 the International GNSS Service (IGS) started to provide the new product of zenith path delay (ZPD) with an accuracy of 1.5-5 mm. However, we found an error in these products up to 30 mm at epochs between 2 days due to the day boundary effect and an average of 16mm RMS for nine days. Our research shows that for reducing the impact, the most critical factor is selecting the initial value for the ZPD, followed by satellite orbit/clock and, finally, the station coordinate values. By choosing an appropriate initial value for ZPD and employing a 3 days orbit/clock, the ZPD error due to the day boundary effect can be reduced to negligible. Meanwhile, the change in the station coordinate value in cm level does not impact the effect.

*Keywords:* Zenith Path Delay, TZD, day boundary effect, GNSS, PPP.

©2021 Vietnam Academy of Science and Technology

### 1. Introduction

When passing through the troposphere, GNSS signals are delayed by about 2.4 m in the direction of the zenith. This delay is called Tropospheric Zenith Delay - TZD or Zenith Path Delay - ZPD. In the troposphere, the influence of dry air on the GNSS signal is about 90% (~ 2.3 m). The remaining 10% is due to water vapor (~ 0.1 m). Although this

delay is much smaller than the effect of the ionosphere, it is difficult to overcome and model due to the mobility of the water vapor component. This is considered a limitation to be overcome in GNSS precise positioning. Especially for precise point positioning applications such as the determination of ground displacement carried out at permanent GNSS stations in Vietnam recently (Nguyen et al., 2020).

On the opposite side, based on GNSS signal, one can process it to extract the zenith

\*Corresponding author, Email: [nnlau@hcmut.edu.vn](mailto:nnlau@hcmut.edu.vn)

path delay and then convert it to the precipitable water vapor for weather forecasting (Duan et al., 1996; Tregoning et al., 1998; Ha and Nguyen, 2005; Nguyen 2012; Huynh and Nguyen, 2014). Vietnam and the Southeast Asia region, located in the equatorial belt, often have ionospheric irregularities, which will reduce the accuracy of ZPD when extracting from GNSS signals (Nguyen Thanh Dung et al., 2021; Dao Tam et al., 2020).

From 2003 the International GNSS (Global

Navigation Satellite System) Service (IGS) started to supply ZPD products by employing a precise point positioning method (PPP) and using the IGS Combined Final orbit and clock product (Zumberge et al., 1997). The new product is wholly independent of individual contributions of ZPD by the Analysis Centers. The key features of the further processing approach for the IGS ZPD product are summarized in Table 1 (Byun and Bar-Sever, 2009; Bar-Sever and Byun, 2010; Bar-Sever et al., 1998; Hackman et al., 2015).

Table 1. Some key features of the processing approach for the IGS ZPD

| Contents               | Values   |
|------------------------|--|
| Software               | GIPSY, BERNESE   |
| GPS orbits and clocks  | IGS Final Combined   |
| Earth orientation      | IGS Final Combined   |
| Antenna phase center   | IGS Convention   |
| Elevation angle cutoff | 7°   |
| Mapping function       | GMF (Boehm et al., 2006)   |
| A priori               | Hydrostatic delay based on altitude (2.3 m at sea level), and 0.1 m for the wet delay  |
| Data time span         | 24 h   |
| Data rate              | 5 min  |
| Estimated parameters   | Receiver clock (white noise), station position (constant), wet zenith delay (random walk with variance of 3 cm/h), atmospheric gradients (random walk with variance of 0.3 cm/h), phase biases (white noise) |

The new IGS ZPD products are reported to have an accuracy of 1.5-5 mm (Byun and Bar-Sever, 2009). However, the authors in the article also admitted that it contains biases due to the day boundary effect. And in the future, they will continue to improve by using weather models to derive a better a priori value of the hydrostatic delay and 30 h arcs to reduce the effect.

Hackman et al. (2015) reported the so-called “day-boundary discontinuities” of about 4-7 mm RMS (depending on location) to appear between parameter values computed at the end of one 24 hr measurement block and the beginning of the next. They also announced that research is ongoing at Technische Universität München to characterize and then minimize these discontinuities.

The accuracy of the IGS ZPD was also confirmed recently by Mendez et al. (2018)

compared with the processing results of some online services. The estimates of two out of the three online PPP services show good agreement (<1 cm) with the IGS ZPD values at the northern and southern hemisphere stations.

In another study by Zang et al. (2020), the authors indicated that the day-boundary discontinuities are due to the IGS products. The averaging of this colored pseudo-range noise induces clock datum changes between daily batches at the level of a few hundred picoseconds to a few nanoseconds. IGS uses daily batches of GPS observations to estimate the precise satellite orbit and clocks. Therefore, there are boundary jumps visible from day to day in the products. PPP is based on the IGS estimates, and therefore PPP and its products such as ZPD may inherit this effect. To prevent ZPD discontinuity at the end-day epochs due to boundary jumps in the

products, it is necessary to interpolate the 2 day orbit and satellite clock corrections in PPP.

Our purpose in this paper is to assess the accuracy of the current IGS ZPD products at epochs between 2 days due to day boundary effects. After that, we will analyze and find out the contribution of the leading causes of the error. And finally, we propose methods to overcome this error.

**2. Data for testing**

While storms or typhoons form, they create sudden precipitable water vapor in the troposphere. This causes the ZPD to increase/decrease significantly compared with the standard value calculated by empirical models. To investigate the ZPD error, mainly

due to the day boundary effect, we selected GNSS data during the 2020 typhoon season from 29/10/2020 to 6/11/2020 in the East Vietnam Sea area and its vicinity (day of the year from 303 to 311). This is one of the stormiest areas in the world. Especially during this time, there was Super Typhoon Goni with a wind speed up to 220 km/h, sweeping directly through PIMO and PTGG stations from October 31, 2020.

We choose 4 permanent GNSS stations belonging to the IGS network. These stations have exact coordinates in ITRF2014. More importantly, they have the IGS ZPD product available for all the days selected above. The locations of the stations are shown in Fig. 1. Some of the GNSS receiver specifications are shown in Table 2.

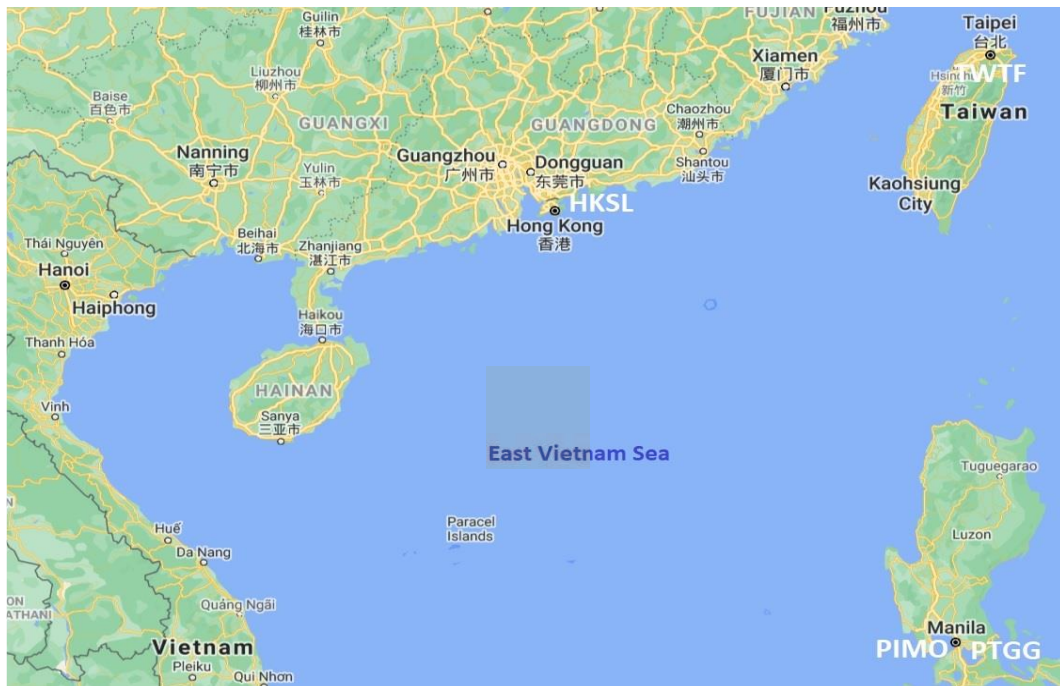


Figure 1. Location of the testing stations

Table 2. Characteristics of GNSS receivers at IGS stations

| No. | Station | Nation or Territorial region | Receiver             | Antenna           |
|-----|---------|------------------------------|----------------------|-------------------|
| 1   | HKSL    | Hong Kong                    | JAVAD TRE G3TH DELTA | LEIAR25.R4 LEIT   |
| 2   | PIMO    | Philippines                  | LEICA GR50           | ASH701945C_M NONE |
| 3   | PTGG    | Philippines                  | JAVAD TRE 3 DELTA    | TRM59800.00 SCIS  |
| 4   | TWTF    | Taiwan                       | SEPT POLARX4TR       | ASH701945C_M SCIS |

**3. Assessment of ZPD biases**

We downloaded the IGS ZPD values of the four stations over the selected period from the website: <http://cddis.gsfc.nasa.gov/gps/products/troposphere/zpd>. For analysis, we plot these values of the PIMO station in Fig. 2.

From the graph, we can see that the enormous ZPD value changes occurred at the end of day 305 and the beginning of day 306 from 2.52 m to 2.68 m that is when Super

Typhoon Goni swept through the station. At the epochs between 2 consecutive days, the IGS ZPD value has a different jump, reaching up to 30 mm. This interruption did not come from a sudden fluctuation of the troposphere, but from the data processing, like information (GPS satellite orbit, GPS satellite clock corrections, ZPD apriori values, station coordinate values, other corrections,...) independently of each day of processing data - also called day boundary effect.

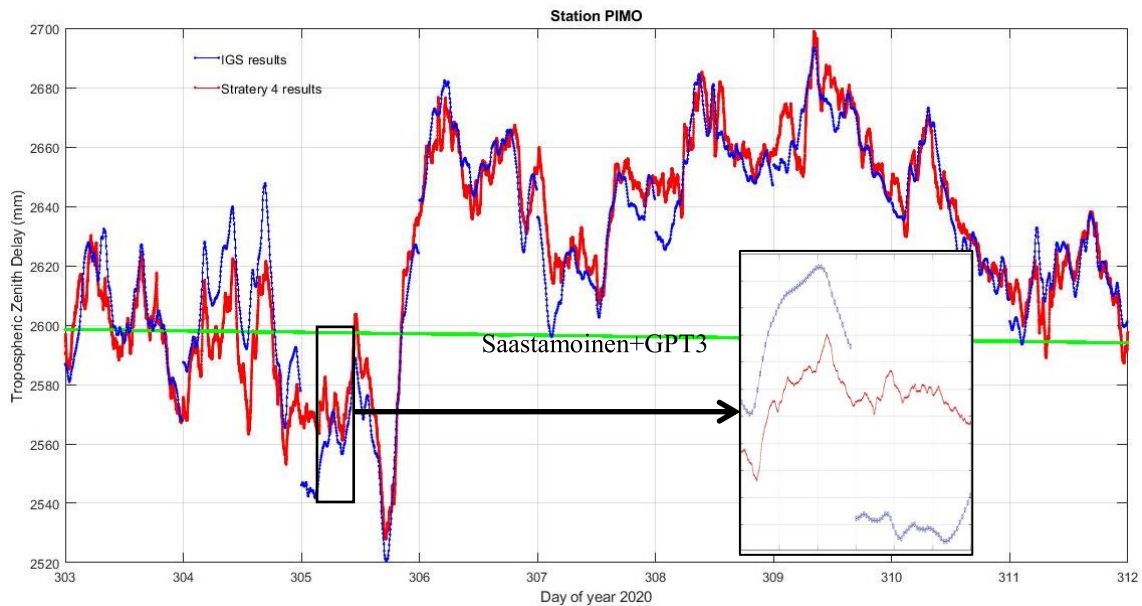


Figure 2. IGS ZPD values (blue) of station PIMO from 29/10 to 6/11/2020

To evaluate the error of IGS ZPD at the epochs between 2 days, we use the extrapolation method to calculate the ZPD value of the standard epoch from 2 days and then get the difference  $\Delta$  of the two extrapolated values (Fig. 3). Assuming the error of the ZPD points and the extrapolation error are ignored, the ZPD error at the interested epoch can be considered as  $\Delta$ . Through testing, we found that using the first-order function to extrapolate 5-minutes IGS ZPD values gave the smallest deviation. We illustrate the  $\Delta$  calculation of the PIMO

station between days 304 and 305 in Table 3.

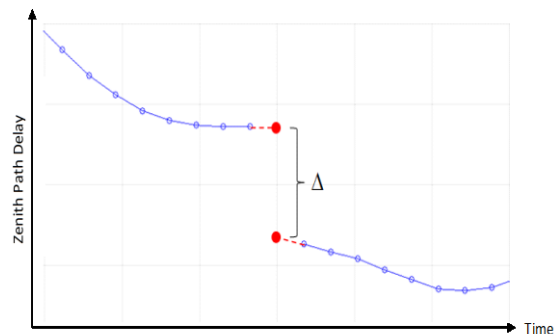


Figure 3. Estimation of ZPD biases between 2 consecutive days

Table 3. Calculation of IGS ZPD error at PIMO between days 304 and 305

| Day of year | ZPD values (mm) |        |              | ZPD error (mm) |
|-------------|-----------------|--------|--------------|----------------|
|             | Epoch1          | Epoch2 | Extrapolated |                |
| 304         | 2577.9          | 2577.5 | 2577.3       | 31.3           |
| 305         | 2546.3          | 2546.1 | 2546.0       |                |

The general error for all days of a station is calculated by the formula:

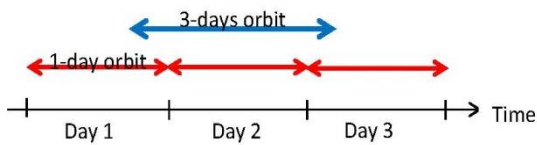
$$RMS = \sqrt{\frac{\sum_{i=1}^n \Delta_i^2}{n}} \quad (1)$$

Applying the above method, we calculate the error of IGS ZPD for 9 days data of PIMO station as 15.7 mm (8.5 mm for PTGG, 5.2 mm for HKSL and 7.9 mm for TWTF). This error is three times higher than the published error of IGS (1.5-5 mm) (Byun and Bar-Sever, 2009) or 4-7 mm reported by Hackman et al. (2015).

**4. Analysis of the causes**

To find out the cause and extent of its effect on the day boundary ZPD error, we will analyze the following possible factors:

- IGS GPS orbit and clock corrections: use 1 day orbit/clock or 3 days orbit/clock to interpolate at times between 2 days



- Priors values of ZPD: Use ZPD values computed from the model (Saastamoinen+GPT3) or estimated values from the last epoch of the previous day

- Station coordinate values: Use separate coordinate values for each day or share common coordinate value for all days. The coordinates in ITRF2014 (Altamimi et al., 2016) for each day are given in Table 4. This is also the value that IGS used to supply the ZPD product. When using common values for

all days, we use the GPS 2130 week solution for the stations.

We set up a Kalman filter with the main features similar to Byun and Bar-Sever (2009). The theoretical basis of ZPD extraction has been summarized in the paper (Nguyen Ngoc Lau, 2012). Some features of our filter are outlined in Table 5.

Comparing the characteristics in Table 5 and Table 1, our processing method differs from IGS only in data rate (the 30s vs. 5 minutes), a priori hydrostatic and wet delay values, and the estimated parameter without receiver clocks, because we use between satellites, differenced measurements. Using this filter, we extracted the ZPD of the four stations in 5 different strategies (named 0 to 4). For each option, we calculate the RMS by formula (1). For strategy 0 alone, we output ZPD by intervals of 5 minutes and 30s. The 5 minute ZPD was used to compare with IGS results. Our processing results are given in Table 6.

Among the five proposed processing strategies, strategy 0 has the closest configuration to the IGS process. The actual results have proved that our 5 minute ZPD has an entirely similar RMS value with IGS ZPD at all four stations. This proves that our filter setup is identical to that of IGS. Also, in strategy 0, the RMS of 30s ZPD always has a value greater than 5 minutes because 30s ZPD values have higher noise. However, we still want to continue working with the 30s ZPD because it has the advantage of giving a smaller gap between two consecutive days. For the 30s of data rate, the last epoch of a day is 23:59:30, only 30 seconds from the first epoch of the next day, instead of 5 minutes data rate. Assuming the day boundary effect is negligible, the shorter the gap, the closer the ZPD of the last epoch of the previous day will be to the ZPD of the first epoch of the next day.

Table 4. Station coordinates in ITRF2014

| Day of year            | Station | X (m)         | Y (m)        | Z (m)        |
|------------------------|---------|---------------|--------------|--------------|
| 303                    | HKSL    | -2393383.102  | 5393860.940  | 2412592.172  |
|                        | PIMO    | -3186293.526  | 5286624.434  | 1601158.392  |
|                        | PTGG    | -3184364.475  | 5291037.231  | 1590413.597  |
|                        | TWTF    | -2994428.629  | 4951309.049  | 2674496.700  |
| 304                    | HKSL    | -2393383.100  | 5393860.931  | 2412592.172  |
|                        | PIMO    | -3186293.509  | 5286624.413  | 1601158.388  |
|                        | PTGG    | -3184364.477  | 5291037.230  | 1590413.600  |
|                        | TWTF    | -2994428.627  | 4951309.048  | 2674496.701  |
| 305                    | HKSL    | -2393383.101  | 5393860.935  | 2412592.170  |
|                        | PIMO    | -3186293.546  | 5286624.460  | 1601158.391  |
|                        | PTGG    | -3184364.489  | 5291037.241  | 1590413.602  |
|                        | TWTF    | -2994428.627  | 4951309.042  | 2674496.698  |
| 306                    | HKSL    | -2393383.098  | 5393860.939  | 2412592.171  |
|                        | PIMO    | -3186293.536  | 5286624.441  | 1601158.397  |
|                        | PTGG    | -3184364.483  | 5291037.244  | 1590413.599  |
|                        | TWTF    | -2994428.624  | 4951309.050  | 2674496.698  |
| 307                    | HKSL    | -2393383.103  | 5393860.934  | 2412592.169  |
|                        | PIMO    | -3186293.531  | 5286624.443  | 1601158.395  |
|                        | PTGG    | -3184364.491  | 5291037.246  | 1590413.601  |
|                        | TWTF    | -2994428.636  | 4951309.051  | 2674496.703  |
| 308                    | HKSL    | -2393383.103  | 5393860.934  | 2412592.167  |
|                        | PIMO    | -3186293.537  | 5286624.435  | 1601158.390  |
|                        | PTGG    | -3184364.486  | 5291037.239  | 1590413.599  |
|                        | TWTF    | -2994428.633  | 4951309.045  | 2674496.698  |
| 309                    | HKSL    | -2393383.105  | 5393860.935  | 2412592.168  |
|                        | PIMO    | -3186293.533  | 5286624.441  | 1601158.392  |
|                        | PTGG    | -3184364.484  | 5291037.245  | 1590413.598  |
|                        | TWTF    | -2994428.635  | 4951309.048  | 2674496.700  |
| 310                    | HKSL    | -2393383.100  | 5393860.932  | 2412592.167  |
|                        | PIMO    | -3186293.522  | 5286624.436  | 1601158.389  |
|                        | PTGG    | -3184364.481  | 5291037.245  | 1590413.595  |
|                        | TWTF    | -2994428.630  | 4951309.052  | 2674496.700  |
| 311                    | HKSL    | -2393383.108  | 5393860.939  | 2412592.170  |
|                        | PIMO    | -3186293.527  | 5286624.426  | 1601158.389  |
|                        | PTGG    | -3184364.485  | 5291037.236  | 1590413.595  |
|                        | TWTF    | -2994428.633  | 4951309.047  | 2674496.697  |
| GPS week 2130 solution | HKSL    | -2393383.1036 | 5393860.9384 | 2412592.1715 |
|                        | PIMO    | -3186293.5306 | 5286624.4356 | 1601158.3930 |
|                        | PTGG    | -3184364.4800 | 5291037.2436 | 1590413.5977 |
|                        | TWTF    | -2994428.6274 | 4951309.0502 | 2674496.7004 |

The results of strategy 1 show that using a 3 day orbit/clock reduces the day boundary effect. However, the reduction is not uniform across stations. The most are PTGG with an improvement of 1-12.6/16.5~32%, and the least are PIMO with only 1-12.6/13.0~3%. The key factor, in this case, is the a priori value of ZPD. When the troposphere has significant fluctuations due to storms,

typhoons, heavy rains ..., the use of meteorological models to compute a priori values of ZPD containing large errors (up to 3-6 cm, see Fig. 1). The larger the deviation from the initial value, the longer it will take for the ZPD to converge to the correct value. This causes the ZPD values in the early epochs to be more erroneous, exacerbating the day boundary effect. Therefore, taking

the estimated ZPD value at the last period of the previous day as the approximate value of the first epoch of the current day will eventually overcome this problem. Strategy 2 shows an improvement of 96-98% at all stations.

Table 5. Some key features of our processing approach

| Contents                                 | Values  |
|--|---|
| Software                                 | PPPC  |
| GPS orbits and clocks                    | IGS Final Combined  |
| Earth orientation                        | IGS Final Combined  |
| Antenna phase center                     | IGS Convention  |
| Elevation angle cutoff                   | 7°  |
| Mapping function                         | GMF (Boehm et al., 2006)  |
| A priori hydrostatic delay and wet delay | Saastamoinen (1973) with meteorological parameters from GPT3  |
| Data time span                           | (Landskron and Böhm, 2018)  |
| Data rate                                | 24 h  |
| Estimated parameters                     | 30s<br>station position (constant), wet zenith delay (random walk with variance of 3 cm/h), atmospheric gradients (random walk with variance of 0.3 cm/h), phase biases (white noise) |

Table 6. Strategies of processing and results

| Strategy                              | Interval | IGS orbit/clock | A priori of ZPD            | Station coordinates | RMS (mm) |      |      |      |
|---------------------------------------|----------|-----------------|----------------------------|---------------------|----------|------|------|------|
|                                       |          |                 |                            |                     | HKSL     | PIMO | PTGG | TWTF |
| IGS                                   |          |                 |                            |                     | 5.2      | 15.7 | 8.5  | 7.9  |
| 0                                     | 5m       | 1 day           | model                      | daily               | 5.0      | 15.9 | 8.2  | 7.7  |
| 0                                     | 30s      | 1 day           | model                      | daily               | 8.6      | 16.5 | 13.0 | 12.0 |
| 1                                     | 30s      | 3 days          | model                      | daily               | 5.8      | 12.6 | 12.6 | 11.5 |
| 2                                     | 30s      | 1 day           | Last epoch of previous day | daily               | 0.33     | 0.25 | 0.22 | 0.40 |
| 3                                     | 30s      | 3 days          | Last epoch of previous day | daily               | 0.03     | 0.05 | 0.05 | 0.03 |
| 4                                     | 30s      | 3 days          | Last epoch of previous day | week solution       | 0.03     | 0.05 | 0.05 | 0.03 |
| Deviations between strategies 3 and 4 |          |                 |                            |                     | 0.96     | 4.85 | 2.19 | 0.90 |

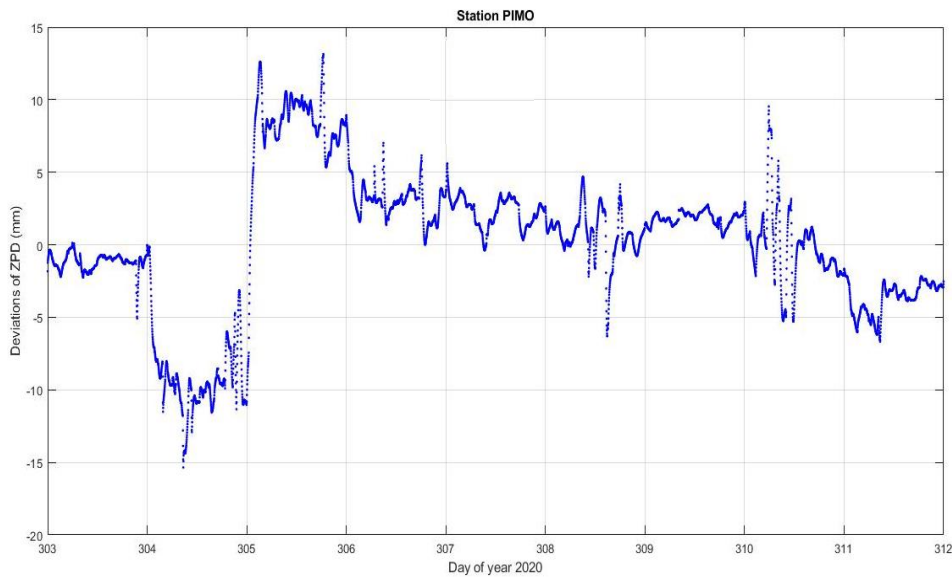


Figure 4. Deviations of ZPD between strategies 3 and 4

Sharing coordinate values for all dates in strategy four did not improve ZPD due to the day boundary effect. This is because the station coordinate values used in the 0-3 strategies differ only a few centimeters between days. This difference is not enough to cause a difference between strategies 3 and 4. However, these two strategies do not give the same ZPD results. In theory, strategy four should provide better ZPD accuracy than 3. Comparing strategies 3 and 4, the RMS of the deviations has the most significant value at PIMO, reaching 4.8 mm (see bottom row of Table 5). Figure 4 shows that the most important difference between strategies 3 and 4 at PIMO station up to 1.5 cm occurred on days 304 and 305. These are also the two days with the largest deviation coordinates compared to more than 2 cm common coordinates.

In summary, the remaining day boundary effect is negligible when applied at the same time, three days orbit/clock, and a priori suitable values for ZPD (strategy 3 or 4). Using accurate station coordinates for all days can improve ZPD accuracy but virtually unchanged the day boundary effect.

## 5. Conclusions

To investigate the error of the current IGS ZPD product due to day boundary effect, we used the GNSS data of the four stations in the East Vietnam Sea area and its vicinity from October 29 to November 6, 2020. Our calculation results show that the ZPD error can be up to 30 mm, and the maximum 9-day RMS value is 15.9 mm at the PIMO station. This error is almost three times higher than the published error of IGS (1.5-5 mm).

To find the cause and overcome the day boundary effect, we have created a Kalman filter with main features similar to IGS (Byun and Bar-Sever, 2009). Using this filter, we analyze the factors that can affect the ZPD, including satellite orbit/clock, a priori values

of ZPD, station coordinate values. Our results show:

- The most influential factor is the a priori value of ZPD. Using the ZPD estimate in the last epoch of the previous day as an approximate value for today's first epoch, the day boundary effect can be reduced to more than 96% at between 2-days epochs.

- The second most influencing factor is the use of satellite orbits/clocks for three days instead of 1 day. This can reduce the day boundary effect by about 3-32%, depending on the station.

- Using the accurate value of the station coordinates can improve the ZPD accuracy but negligibly affects the day boundary effect.

## References

- Altamimi Z., P. Rebischung, L. Métivier, X. Collilieux, 2016. ITRF2014: A new release of the International Terrestrial Reference Frame modeling nonlinear station motions. *J. Geophys. Res. Solid Earth*, 121, 6109-6131. Doi: 10.1002/2016JB013098.
- Bar-Sever Y.E., Kroger P.M., Borjesson J.A., 1998. Estimating horizontal gradients of tropospheric path delay with a single GPS receiver. *J. Geophys. Res.*, 103(B3), 5019-5035.
- Bar-Sever YE, Sung Byun, 2010. <https://lists.igs.org/pipermail/igsmail/2010/000132.html>.
- Boehm J., A. Niell, P. Tregoning, H. Schuh, 2006. Global Mapping Function (GMF): A new empirical mapping function based on numerical weather model data. *Geophysical Research Letters*, 33, L07304. Doi: 10.1029/2005GL025546, 2006.
- Byun S.H., Yoaz E. Bar-Sever, 2009. A new type of troposphere zenith path delay product of the international GNSS service. *Journal of Geodesy*, 83, 367-373. Doi: 10.1007/s00190-008-0288-8.
- Dao Tam, Minh L.H., Carter B., Le Q., Trinh T.T., Phan B.N., Otsuka Y., 2020. New observations of the total electron content and ionospheric scintillations over Ho Chi Minh City. *Vietnam Journal of Earth Sciences*, 42(4), 320-333. <https://doi.org/10.15625/0866-7187/42/4/15281>.



- Ha Minh Hoa, Nguyen Ngoc Lau, 2005. Ability to use GPS satellite signals on permanent stations to determine air humidity in the troposphere. The 9<sup>th</sup> Scientific Workshop of the Institute of Meteorology and Hydrology. Hanoi. Vietnam.
- Hackman C., Guergana Guerova, Sharyl Byram, Jan Dousa, Urs Hugentobler, 2015. International GNSS Service (IGS) Troposphere Products and Working Group Activities. FIG Working Week 2015 From the Wisdom of the Ages to the Challenges of the Modern World Sofia. Bulgaria, 17-21 May 2015.
- Huynh Nguyen Dinh Quoc, Nguyen Ngoc Lau, 2014. Comparison of PWV values derived by GNSS and by radiosonde at Tan Son Hoa station, Ho Chi Minh City. *Journal of Geodesy and Cartography*, 19, 21-28 (in Vietnamese).
- Jingping Duan, Michael Bevis, Peng Fang, Yehuda Bock, Steven Chiswell, Steven Businger, Christian Rocken, Frederick Solheim, Terasa van Hove, Randolph Ware, Simon McClusky, Thomas A. Herring, Robert W. King, 1996. Meteorology: direct estimation of the absolute value of precipitable water. *Journal of Applied Meteorology*, 35, 830-838.
- Landskron D., Johannes Böhm, 2018. VMF3/GPT3: refined discrete and empirical troposphere mapping functions. *Journal of Geodesy*, 92, 349-360. <https://doi.org/10.1007/s00190-017-1066-2>.
- Mendez J. Astudillo, Lawrence Lau, Yu-Ting Tang, Terry Moore, 2018. Analysing the Zenith Tropospheric Delay Estimates in On-line Precise Point Positioning (PPP) Services and PPP Software Packages. *Sensors* 2018, 18, 580. Doi: 10.3390/s18020580.
- Nguyen Ngoc Lau, 2012. Determination of PWV by using GPS precise point positioning. *Journal of Meteorology and Hydrology*, 614, 40-44 (in Vietnamese).
- Nguyen Ngoc Lau, Coleman R., Hoa H.M., 2020. Determination of tectonic velocities of some continuously operating reference stations (CORS) in Vietnam 2016-2018 by using precise point positioning. *Vietnam Journal of Earth Sciences*, 43(1), 1-12. <https://doi.org/10.15625/0866-7187/15571>.
- Nguyen Thanh Dung, Le Huy M., Amory-Mazaudier C., Fleury R., Saito S., Nguyen Chien T., Pham Thi Thu H., Le Truong T., Nguyen Thi M., 2021. Characterization of ionospheric irregularities over Vietnam and adjacent region for the 2008-2018 period. *Vietnam Journal of Earth Sciences*. <https://doi.org/10.15625/2615-9783/16502>.
- Paul Tregoning, Reinout Boers, Denis O'Brien, Martin Hendy, 1998. Accuracy of absolute precipitable water vapour estimates from GPS observations. *Journal of Geophysical Research*, 103(D22), 28701-28710.
- Saastamoinen J., 1973. Contribution to the theory of atmospheric refraction. *Bulletin Geodesique*, 107, 13-34.
- Zhang X., Ji Guo, Yonghui Hu, Dangli Zhao, Zaimin He, 2020. Research of Eliminating the Day-Boundary Discontinuities in GNSS Carrier Phase Time Transfer through Network Processing. *Sensors* 2020, 20, 2622. Doi: 10.3390/s20092622.
- Zumberge J.F., Heflin M.B., Jefferson D.C., Watkins M.M., Webb F.H., 1997. Precise point positioning for the efficient and robust analysis of GPS data from large networks. *J. Geophys. Res.*, 102(B3), 5005-5017.